Journal of Environmental Management 189 (2017) 98–108

Contents lists available at ScienceDirect

Journal of Environmental Management

journal homepage: www.elsevier.com/locate/jenvman

Research article

Iron removal, energy consumption and operating cost of electrocoagulation of drinking water using a new flow column reactor

Khalid S. Hashim [a, b, *], Andy Shaw [a], Rafid Al Khaddar [a], Montserrat Ortoneda Pedrola [a], David Phipps [a]

[a] School of Civil Engineering, Liverpool John Moores University, Liverpool, UK
[b] Department of Environment Engineering, Babylon University, Babylon, Iraq

ARTICLE INFO

Article history:
Received 7 October 2016
Received in revised form
12 December 2016
Accepted 13 December 2016

Keywords:
Iron
Electrocoagulation
Aluminium
Perforated electrodes
Empirical model
Operating cost

ABSTRACT

The goal of this project was to remove iron from drinking water using a new electrocoagulation (EC) cell. In this research, a flow column has been employed in the designing of a new electrocoagulation reactor (FCER) to achieve the planned target. Where, the water being treated flows through the perforated disc electrodes, thereby effectively mixing and aerating the water being treated. As a result, the stirring and aerating devices that until now have been widely used in the electrocoagulation reactors are unnecessary.

The obtained results indicated that FCER reduced the iron concentration from 20 to 0.3 mg/L within 20 min of electrolysis at initial pH of 6, inter-electrode distance (ID) of 5 mm, current density (CD) of 1.5 mA/cm^2, and minimum operating cost of 0.22 US $/m^3. Additionally, it was found that FCER produces H_2 gas enough to generate energy of 10.14 kW/m^3.

Statistically, it was found that the relationship between iron removal and operating parameters could be modelled with R^2 of 0.86, and the influence of operating parameters on iron removal followed the order: $C_0 > t > CD > pH$. Finally, the SEM (scanning electron microscopy) images showed a large number of irregularities on the surface of anode due to the generation of aluminium hydroxides.

Crown Copyright © 2016 Published by Elsevier Ltd. All rights reserved.

1. Introduction

Iron is one of the most common elements in nature as it represents about 5% of the earth's crust (Ityel, 2011), and it can be found in fresh waters at a concentration of 0.5–50 mg/L (WHO, 2004). This element naturally exists in water in different states: soluble state (as ferrous Fe^{2+}), insoluble state (ferric hydroxide Fe^{3+}), bacterial state, and organic state (Chaturvedi and Dave, 2012). In addition to the natural occurrence of iron, many industries, such as mining and steel industries, contribute to the occurrence of iron in water (Ghosh et al., 2008a).

Although iron has been classified as a secondary contaminant as it is not harmful for human beings, it causes aesthetic problems such as taste issues, turbidity, and discolouration (Phadke, 2014). Moreover, presence of iron motivates the bacterial growth (iron bacteria such as *Gallionella*, and *Leptothrix*), which block the plumbing in consequence (Ityel, 2011; Chaturvedi and Dave, 2012). However, iron represents an essential element for human heath, where the daily intake of iron is recommended to be between 10 and 50 mg depending on the person's gender, age, physiological status, and the bioavailability of iron (WHO, 2004). Based on these considerations, the World Health Organization (WHO) limits the iron concentration in drinking water to 0.3 mg/L (WHO, 2004).

Indeed, a wide spectrum of treatment methods have been practised to remove iron from water such as oxidation by aeration, chemical oxidation, biological removal, ion exchange, adsorption, membrane filtration, and electrocoagulation (Ghosh et al., 2008a; Ityel, 2011; Chaturvedi and Dave, 2012; Phadke, 2014).

In comparison with other methods, the EC method bears many attractive advantages such as it is simple to install and operate, requires no chemical handling, and there is the possibility of complete automation and integrating with other methods. It produces fewer total dissolved solids, and it has a large treatment capacity and a relatively shorter treatment time (Ghosh et al., 2013; Khandegar and Saroha, 2013; Kamaraj and Vasudevan, 2015; Aghdam et al., 2015). Furthermore, as advancements in the

* Corresponding author. School of Civil Engineering, Liverpool John Moores University, Liverpool, UK.
E-mail address: k.s.hashim@2013.ljmu.ac.uk (K.S. Hashim).

http://dx.doi.org/10.1016/j.jenvman.2016.12.035
0301-4797/Crown Copyright © 2016 Published by Elsevier Ltd. All rights reserved.

production of alternative clean energy resources are made, use of the EC method will become possible even in rural areas (Chaturvedi and Dave, 2012), where sufficient energy can be driven from an attached solar panel (Deokate, 2015; García-García et al., 2015).

However, the EC method still has a clear deficiency in the variety of reactor design (Un et al., 2013), as most of the electrocoagulation reactors still rely on parallel arrangement of simple plate electrodes inside a container. In addition, the availability of models for the EC process is also limited, which represents a limitation in the understanding of this treatment method (Kuokkanen, 2016).

2. Aims and objectives

The current study has been devoted to fill a part of the gaps in the literature. The objectives of this study are:

- Suggestion of a new configuration for an electrocoagulation reactor (FCER) which employs a perforated plate flow column (which are widely used in chemical industries).
- Investigate the ability of FCER to remove pollutants from drinking water (iron as a case study). The influence of key operating parameters, such as electrolysis time (t) (0–45 min), initial pH value (4–8), current density (CD) (1, 1.5, and 2 mA/cm^2), inter-electrode distance (ID) (5–20 mm), initial iron concentration (C_0) (20–60 mg/L), and water temperature (T) (10–30 °C), will be taking into accounts.
- Development of an empirical model to reproduce the performance of FCER in terms of iron removal.
- Carry out a preliminary economic study to estimate the operating cost of iron removal from drinking water by FCER.
- Estimate the produced amount of hydrogen gas (H_2), during iron removal, and the yieldable energy from this gas.
- Investigate of the influence of the EC process on morphology of the surface of the aluminium anodes using the SEM (scanning electron microscopy) technology.

3. Brief description of reaction mechanism

The concept of the electrocoagulation method is the in-situ generation of the coagulants as the sacrificial metallic anode dissolves due to the applied current, while the cathode generates hydrogen gas that floats the pollutants (Essadki et al., 2009). The electrode material is selected depending on many parameters such as cost, oxidation potential, and targeted pollutant. Although different materials such as steel (Genc and Bakirci, 2015), graphite (Gao et al., 2013), zinc (Vasudevan et al., 2012b), and iron (Ye, 2016), have been used as electrodes in the EC reactors, it has been reported that iron and aluminium are the most effective and successful electrode materials (Chaturvedi and Dave, 2012).

When aluminium (Al) is used as electrodes, the anode produces the Al^{3+} ions; these aluminium cations instantly undergo more reactions to form different types of monomeric materials such as $Al(OH)^{+2}$ and polymeric species such as $Al_{13}O_4(OH)_{24}^{7+}$, which immediately coagulate to form flocs (Ghosh et al., 2008a; Essadki et al., 2009). These reactions can be summarised by the following equations (Ghosh et al., 2008b; Chaturvedi, 2013):

Anode:

$$Al_{(s)} \rightarrow Al^{3+}_{(aq)} + 3e \quad (1)$$

Cathode:

$$3H_2O + 3e \Leftrightarrow \frac{3}{2}H_2\uparrow + 3OH^- \quad (2)$$

Then, Al^{3+} and OH^- ions react to generate $Al(OH)_3$:

$$Al^{3+} + 3H_2O \rightarrow Al(OH)_3 + 3H^+ \quad (3)$$

Reaction between Al (III) and hydroxide ions results in formation of different aluminium monomeric and polymeric species, such as $Al(OH)^{+2}$, $Al_2(OH)_2^{4+}$, $Al_7(OH)_{17}^{4+}$, and $Al_{13}O_4(OH)_{24}^{7+}$, which transform, according to complex precipitation kinetics, into $Al(OH)_{3(S)}$, (Ghosh et al., 2008a).

It is believed that aluminium hydroxide flocs, $Al(OH)_3$, are responsible for the adsorption and precipitation of the dissolved pollutants, while the small hydrogen bubbles that blow around the cathode are responsible for the floatation of pollutants (Adhoum et al., 2004; Ghosh et al., 2008a). The dominant path of pollutants' removal, sedimentation or floatation, during the last stage is determined by the applied current, where the majority of the dissolved pollutants are removed by floatation at high currents, while sedimentation is the predominant path at low currents (Maximova and Dahl, 2006; Chaturvedi and Dave, 2012).

Generally, iron exists in water in the ferrous form which, in the presence of oxygen and pH below 6.5, immediately undergoes oxidation reactions as follows (Chaturvedi and Dave, 2012):

$$Fe^{2+} + \left(\frac{1}{4}\right)O_2 + H^+ \Leftrightarrow Fe^{3+} + \left(\frac{1}{2}\right)H_2O \quad (4)$$

Additionally, iron ions react with hydroxide ions to form $Fe(OH)_3$ according to the following reactions (Ghosh et al., 2008a):

Bulk

$$H_2O \Leftrightarrow H^+ + OH^- \quad (5)$$

$$NaCl \Leftrightarrow Na^+ + Cl^- \quad (6)$$

$$Fe^{2+} + 2Cl^- \Leftrightarrow FeCl_2 \quad (7)$$

$$FeCl_2 + 2OH^- \Leftrightarrow Fe(OH)_2\downarrow + 2Cl^- \quad (8)$$

$$H^+ + Cl^- \Leftrightarrow HCl \quad (9)$$

Anode

$$2Cl^- \Leftrightarrow Cl_2\uparrow + 2e \quad (10)$$

4. Materials and methods

4.1. Experimental set up

A new cylindrical electrocoagulation reactor (FCER) has been designed basing on the innovative use of a perforated-plate flow column. FCER consists of a flow column containing 6 aluminium perforated discoid plates, 5.2 cm in radius and 1 mm in thickness of 99.5% purity provided by LJUM laboratories, Fig. 1. These perforated electrodes were stacked vertically within the reaction vessel with the plane of each plate parallel and perpendicular to the direction of flow. Each electrode had the holes offset from the one above it to ensure that the water will flow in a convoluted path in order to increase mixing efficiency. These plates are held in the required position, inside a hollow Perspex cylinder 25 cm in height and 10.5 cm in diameter, using PVC rods and spacers. The PVC rods are

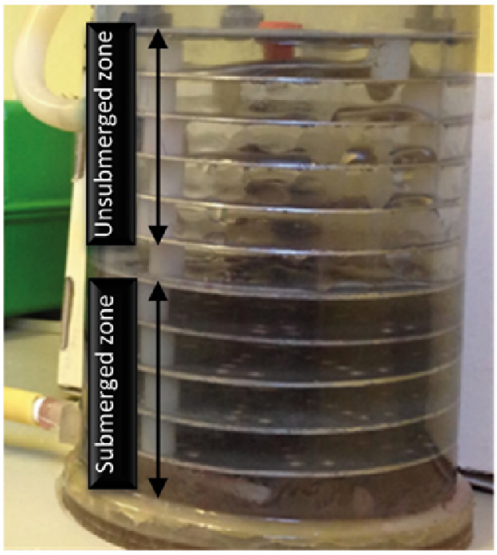


Fig. 1. Flow column EC reactor (FCER).

movable to exclude the accumulated air bubbles, which significantly influence the electrical resistance and the energy consumption as consequence (Gao et al., 2013), on the electrodes during the electrolysis process. The upper unsubmerged electrodes were used as water diffusers (no electric current was applied to them), Where, these unsubmerged electrodes convert the mass water flow into droplets that maximises the contact area between water being treated with the ambient air, which in turn enhances the aeration process. While water mixing process takes place in both submerged and unsubmerged zones.

A peristaltic pump (Watson Marlow type, model: 504U) was used to pump the water. The electrical current was supplied by a rectifier (HQ Power; Model: PS 3010, 0–10 A, 0–30 V). This bench scale system was provided with a thermometer, conductivity, and pH sensor (all of them built on meter type: Hanna; Model: HI 98130).

4.2. Reagents and chemicals

All chemicals, of ≥99% purity, were supplied by Sigma-Aldrich, and used as supplied. Stock synthetic water solution containing 300 mg/L iron was prepared by dissolving 1.493 g of $FeSO_4 \cdot 7H_2O$ in deionised water. Samples of lower concentrations were prepared by dilution from this stock solution. The initial pH of the prepared samples was adjusted to the desired value, between 4 and 8, using 1 M HCl or 1 M NaOH solutions. All the runs were commenced with the water at room temperature (20 ± 1 °C) except those sets for the investigation of temperature effects and water conductivity. The latter parameter was adjusted to 0.32 mS/cm using NaCl salt. At the end of the run, the electrodes were washed carefully with HCl acid and then rinsed with deionised water to remove impurities from the surfaces.

4.3. Procedures and analysis

The electrolysis was commenced by dipping the aluminium electrodes in 0.5 L of freshly prepared sample and connecting them directly to the corresponding anode and cathode in the power source. To monitor the progress of iron removal process, samples of 5 mL were collected from the reactor at 5-min intervals during the course of the experiment and filtered with 0.45 μm filters (Sigma-Aldrich) to separate the unwanted sludge. The residual iron concentration was measured using an atomic absorption spectrophotometer (Thermo Scientific, Model: ICE 3300) which depends on the reflection and absorption of the wavelengths. Conductivity and pH of the collected samples were measured using a Hanna meter (Model: HI 98130). Initial water temperature was adjusted to the required value using a water bath (Nickel-Electro: Clifton) and ice bed. The removal efficiency (RE %) was calculated as follows:

$$RE\% = \frac{C_0 - C_f}{C_f} \times 100\% \tag{11}$$

where C_0 and C_f are the influent and effluent concentrations of iron, in mg/L, respectively. While the energy consumption (E) was determined using the following equation (Ghosh et al., 2011; Un et al., 2013):

$$E = \frac{I*V*T}{Vol.} \tag{12}$$

where E is the electrical energy consumption (kWh/m^3), I is the current (A), V is the potential (V), t is the electrolysis time (hrs), and $Vol.$ is the volume of solution (m^3).

4.4. Statistical analysis

Multiple regression is a family of techniques that enables the user to assess the relationship between one dependant variable (DV) and a set of independent variables (IVs). This technique allows more complex investigation of the interrelationship among several variables, and it encompasses standard, hierarchical, and stepwise multiple regression, but the most popular one is standard multiple regression (Pallant, 2005). The general regression equation is (Tabachnick and Fidell, 2001):

$$Y = A + B_1X_1 + B_2X_2 + \ldots + B_kX_k \tag{13}$$

where Y is the predicted value of the dependant variable, A represents the Y intercept, B_k are the regression coefficients, and X_s are the independent variables. To increase the accuracy of this equation, a random error coefficient (ε) was added to it (Mustapha and Abdu, 2012):

$$Y = A + B_1X_1 + B_2X_2 + \ldots + B_kX_k + \varepsilon \tag{14}$$

The removal efficiency of a pollutant, using the EC method, is a function of the influence of several operating parameters such as t, initial pH, CD, T, C_0 and ID (Emamjomeh and Sivakumar, 2005; Fouad et al., 2009; Un et al., 2013; Genc and Bakirci, 2015), which could be expressed by the following equation:

$$Re\%\ of\ a\ pollutant = f(t,\ pH,\ CD,\ T, C_0,\ \ldots etc) \tag{15}$$

In the current study, the influence of t, initial pH, CD, T, ID, and C_0 the performance of FCER in terms of iron removal was investigated. Hence, iron removal, in the current project, could be expressed as follows:

$$Re\%\ of\ iron = f(t, pH, CD, T, C_0) \tag{16}$$

In order to develop a standard multiple regression model based on the formula stated above, the following three steps are essential (Pallant, 2005):

Step 1: Check the assumptions of the multiple regression, which are:

A. Generalisability

Size of the studied data determines the generalisability of the built model by the multiple regression techniques, as the latter cannot be performed on small datasets (Pallant, 2005). Indeed, the minimum required number of observations to build a generalizable model can be calculated using the following formula (Tabachnick and Fidell, 2001):

$$N > 50 + 8m \tag{17}$$

where N is the sample size, and m is the number of independent parameters that will be used in the multiple regression.

B. Multicollinearity

Existence of multicollinearity, which refers to the correlation among the independent parameters (IVs), within the studied data negatively influences the determinations regarding individual predictors (Tabachnick and Fidell, 2001). The existence of multicollinearity within the collected observations could be detected by calculating the tolerance value, where small tolerance values (<0.1) indicate the existence of the multicollinearity (O'brien, 2007):

$$Tolerance = 1 - R^2 \tag{18}$$

where R^2 is the coefficient of determination of a regression.

C. Outliers

Outlier can be define as an observation that "seems" to be incompatible with other observations in the data set (Tabachnick and Fidell, 2001). The conclusions drawn from the statistical analysis can be strongly influenced by outliers, therefore both DV and the IVs must be screened to detect the extreme values before performing the multiple regression (Pallant, 2005). Statistically, detection of the outliers in the studied sample could be achieved by determining the Mahalanobis distances, which must be less than the critical values listed in Table 1 (Pallant, 2005).

D. Normality, linearity, and homoscedasticity of residuals

These terms relate to the nature of the variables' relationship and the scores' distribution. Where normality indicates that the residuals are normally distributed around the predicted DV, linearity means the residuals show a straight relationship with the predicted DV, and homoscedasticity means the variance in the relationship between the IVs and the DV is the same across all magnitudes of the IVs (Pallant, 2005). The scatterplot provides the required information to check these assumptions, where it is expected, in normal distribution, that less than 1% of the standardised residual values of the observations exceeds the range of 3.0 to −3.0 (Pallant, 2005).

Step 2: Evaluating the contribution of each independent variable.

In this step, the contribution of each individual IV to the generated model will be measured by determining its statistical significance (p). This test indicates whether this IV makes a statistically significant contribution to the generated model or not. Generally, any IV with a significance value less than 0.05, will make a significant contribution to the multiple regression model, while an IV with significance value greater than 0.05 can be omitted from the model as it does not play a significant role (Pallant, 2005).

In this study, SPSS-23 package was used to analyse the data and to construct the empirical model.

Step 3: Evaluating the model

This step concerns the ability of the suggested model to explain the variation in the DV (Pallant, 2005). The coefficient of determination (R^2) is a proper tool to achieve this goal, as it is a measure of how many data points fall within the results of the line generated by the regression model. The R^2 goes on a 0–1 scale: the higher the R^2, the higher the accuracy of the regression model; this coefficient can be calculated using the following equation (Tabachnick and Fidell, 2001):

$$R^2 = SS_{reg}/SS_Y \tag{19}$$

where SS_{reg}, and SS_y are the sum of squares for regression and the total sum of squares respectively. In addition, the statistical significance of the result (Sig) should be checked and its maximum value must be less than 0.05 (Pallant, 2005).

4.5. Operating cost

Operating cost is an elemental parameter in any treatment method as it determines the applicability of that method (Ozyonar and Karagozoglu, 2011). For commercial purposes, the operating cost includes the costs of energy, material (electrodes), chemicals, labour, maintenance, sludge handling, and construction (fixed cost) (Kobya et al., 2009). However, for lab scale units the cost of energy and electrode material are the major components of the operating cost, which can be calculated using the following equation (Kobya et al., 2009; Ozyonar and Karagozoglu, 2011):

$$OC = C_{energy} + C_{electrode} \tag{20}$$

where C_{energy}(kWh/m^3), and $C_{electrode}$ (kg of Al/m^3) are the consumed quantities of energy and material of electrodes per cubic meter of water.

4.6. Estimating the produced hydrogen gas and the yieldable energy from this gas

Hydrogen gas (H_2), which is an eco-friendly and high energy fuel, is the main by-product of the EC method (Eker and Kargi, 2010; Nasution et al., 2011; Lakshmi et al., 2013). In fact, harvesting of H_2 gas is one of the most important advantages of the EC technology. For instance, Phalakornkule et al. (2010) found that about 5.8 to13% of the required electrical energy to perform the EC cell could be obtained from recycling the H_2 gas produced.

The emitted amount of H_2 gas from an EC unit could be estimated using the following formula (Phalakornkule et al., 2010):

Table 1
Critical values for the Mahalanobis distances.

Number of IVs	Critical value	Number of IVs	Critical value	Number of IVs	Critical value
2	13.82	*4*	18.47	*6*	22.46
3	16.27	*5*	20.52	*7*	24.32

Source: Pallant (2005).

$$Q_{H_2} = \frac{CD.\ A.\ t\ .\ H}{F} \quad (21)$$

where, Q_{H_2}, CD, A, t, H, and F are the quantity of the emitted amount of H_2 gas (mole), applied current density in (A/m^2), effective surface area of electrodes (m^2), treatment time (sec), number of hydrogen molecules (1/2), and Faraday's constant (96,500), respectively. The produced amount of H_2 could be expressed in volumetric units using the following ideal gas law (Woody, 2011):

$$pV = nRT \quad (22)$$

where, p, V, n, R, and T represent pressure (kPa), volume (L), moles of gas, gas constant (8.314 J/kmole at atmospheric pressure), and gas temperature (K), respectively.

While the yieldable energy from the H_2 gas could be estimated using the following formula (Phalakornkule et al., 2010):

$$E_{H_2} = m\left(0.244\frac{MJ}{mole}\right) \quad (23)$$

where E_{H_2}, and m are the energy yield (MJ), and amount of H_2 gas (mole), respectively. It is noteworthy to highlight that each 3.6 MJ is enough to produce 1.0 kWh (Phalakornkule et al., 2010).

4.7. Scanning electron microscopy characterisation of electrodes

A SEM investigation was carried out using an electron microscopy (Model: Quanta 200) to explore the influence of EC process on the morphology of the surface of the aluminium anode. In this investigation, the surface of virgin and electrolysed square pieces (9 * 9 mm) of the aluminium anode were carefully cleaned and dried, and then characterised by the scanning electron microscopy.

5. Results and discussion

5.1. Experimental work

5.1.1. Influence of initial pH

pH is used as a measure of hydrogen ions' concentration (H^+), and it can be calculated by the negative logarithm of the concentration of H^+ ions (Lim, 2006). This parameter significantly influences the performance of EC units as it governs the speciation of aluminium hydroxides (Emamjomeh and Sivakumar, 2009; García-García et al., 2015).

To investigate the influence of the initial pH on iron removal using FCER, sets of batch experiments were commenced by adjusting the initial pH of synthetic water samples to the required value (from 4 to 8) using 1 M HCl or 1 M NaOH solutions. While the initial Fe-concentration, CD, and ID were kept constant at 20 mg/L, 1.5 mA/cm^2, and 5 mm respectively.

Fig. 2 shows that, after 20 min of electrolysis, the residual iron concentration decreased gradually as the initial pH increased from 4 to 6 to reach its minimum level, about 1%, at a pH of 6. A slight increase was observed as the initial pH increased from 6 to 7. Then the residual iron concentration increased to the vicinity of 6% as the initial pH increased to 8. This change of iron removal with the initial pH could be mainly attributed to the predominant species of aluminium, where in alkaline and acidic conditions; the prevailing species have low adsorption capacity for iron. While, in the neutral or slight alkaline range of pH, the predominant species have high adsorption capacity for iron ions (Ghosh et al., 2008a; Emamjomeh and Sivakumar, 2009; Un et al., 2013).

Thus, in the current project, the rest of the experiments were carried out at an initial pH of 6.

5.1.2. Influence of current density

Faraday's Law (Equation (24)) highlights a fact that the CD highly influences the coagulant dosage, and the removal efficiency in consequence.

$$X = \frac{(I)(t)(m)}{(Z)(F)} \quad (24)$$

X is the released coagulants from the anode (g), I the applied current in amperes, t electrolysis time (second), M is the molecular weight (26.98 g/mol), Z the number of electron, and F is Faraday's constant (96487 C/mol).

Moreover, the CD determines other parameters that can influence the performance of the EC units such as the floc's growth and size and generation rate of bubbles (Un et al., 2009; Gao et al., 2010; Phadke, 2014).

The influence of CD on iron removal was investigated by the electrolysis of several 20 mg/L iron containing water samples at different CDs (1, 1.5, and 2 mA/cm^2), when the initial pH, and ID were kept constant at 6 and 5 mm, respectively.

The obtained results, Fig. 3-(A), indicated that the higher CD was, the more rapid the iron removal was. Where, it can be seen from this figure that, after 20 min of electrolysis, the residual iron concentration decreased from 6.9% to about 0.1% as the CD increased from 1 to 2 mA/cm^2. This could be attributed, according to Faraday's Law, to the fact that the dissolved coagulants increased as the current density increased. As the coagulants increased, the number of available active sites increased correspondingly, and enhanced iron removal as a consequence (Zhu et al., 2007; Chaturvedi and Dave, 2012).

However, Fig. 3-(B) shows that when CD increased from **1**.0 to 2.0 mA/cm^2, the energy consumption significantly increased from 1.32 to 6.65 kWh/m^3, respectively.

Thus, in this investigation, it might be reasonable to infer that the CD of 1.5 mA/cm^2 is the best value to commence the rest of experiments.

5.1.3. Influence of the inter-electrode distance

The inter-electrode distance (ID) plays a key role in the determination of energy consumption and the removal of pollutants in the EC units due its influence on the ohmic resistance (Mameri et al., 1998; Mohora et al., 2012). The influence of the ID on the iron removal was explored by changing the gap between electrodes from 5 to 10 and 20 mm, when the C_0, CD, and initial pH were kept constant at 20 mg/L, 1.5 mA/cm^2, and 6, respectively.

It was found that the iron removal is reversely proportional to the ID, Fig. 4-(A). For instance, after 10 min of electrolysis, iron removal decreased from 66.2% to 37.4% as the ID increased from 5 to 20 mm, respectively. Moreover, it has been noticed that increasing the gap between electrodes negatively influenced the energy consumption of the EC cell. Where, Fig. 4-(B) shows that the energy consumption has increased from 3.22 to 7.3 kWh/m^3 as the ID increased from 5 to 20 mm, respectively.

This could explained by the fact that if the ID increases then both the resistance and the growth of the passive anodic film will also increase. Therefore the current will decrease and the amount of floc formed will likewise decrease, hence the efficiency will change (Mameri et al., 1998; Ghosh et al., 2008a).

However, a very short ID is not recommended as the generated flocs can be degraded by collision with each other due to high electrostatic attraction (Daneshvar et al., 2004; Khandegar and Saroha, 2013). Additionally, in this study, short IDs were avoided as, practically, excluding the accumulated air bubbles between

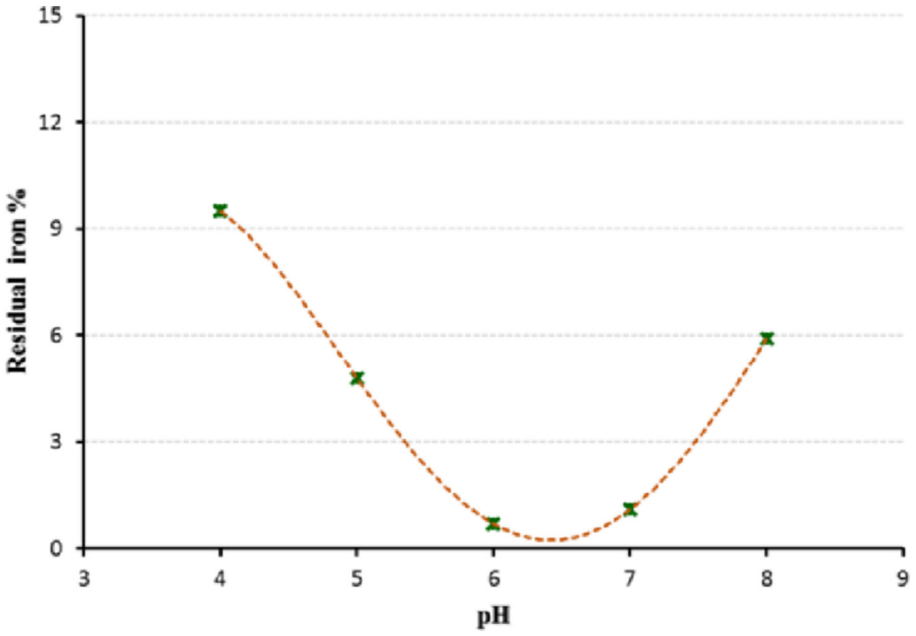


Fig. 2. Effect of initial pH on iron removal.

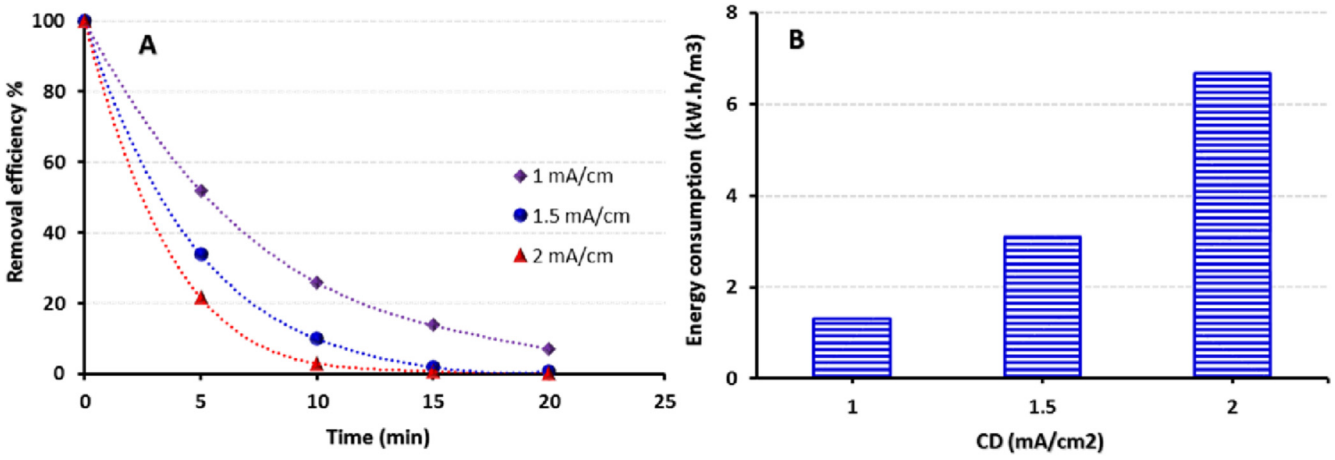


Fig. 3. Effects of CD on: (A) Iron removal efficiency, (B) Energy consumption.

electrodes became more difficult, which negatively influenced the energy consumption. It is reasonable therefore, in the current investigation, to maintain the ID at 5 mm.

5.1.4. Influence of water temperature (T)

The temperature of the solution influences the electrocoagulation rate due to the increasing mobility of ions and collision rate (Fouad et al., 2009; Attour et al., 2014), the activity of the adsorbent surface (Vasudevan et al., 2012c), the dissolution rate of the electrodes, which relates to the formation rate of hydroxyl ions (Song et al., 2007; Vepsäläinen et al., 2009). Additionally, water conductivity increases with temperature (Zaroual et al., 2009; Gao et al., 2010), whereas water viscosity decreases (Fouad et al., 2009; Gao et al., 2010). However, increasing water temperature adversely influences the performance of the EC method as the solubility of precipitates increases at high temperatures (El-Naas et al., 2009; Fouad et al., 2009). Moreover, increasing the collision rate between flocs might degrades them (Daneshvar et al., 2004; Khandegar and Saroha, 2013).

In the present study, influence of water temperature on iron removal was investigated at 10, 20, 30, and 40 ^{0}C. Experiments in which pH of 6, ID of 5 mm, and CD of 1.5 mA/cm^2 were kept constant indicated that increasing water temperature, within the studied range, slightly enhanced iron removal and energy consumption. Where, Fig. 5-(A) shows that, after 15 min of electrolysis, the residual iron decreased from 5.7% to 0.3% as the temperature increased from 10 to 40 ^{0}C. This could be attributed to the fact, as mentioned before, that increasing water temperature enhances the anodic dissolving rate, collision rate between aluminium hydroxide and colloids, pore size on the adsorbents surface, which in turn increases the removal efficiency (Yilmaz et al., 2008; Fouad et al., 2009; Vasudevan et al., 2012c).

In terms of energy consumption, it was noticed that the energy consumption is inversely proportional to the water temperature. Fig. 5-(A) shows that the energy consumption decreased from about 3.4 kWh/m^3 at 10 ^{0}C to 2.5 at 40 ^{0}C. The slight decrease in the

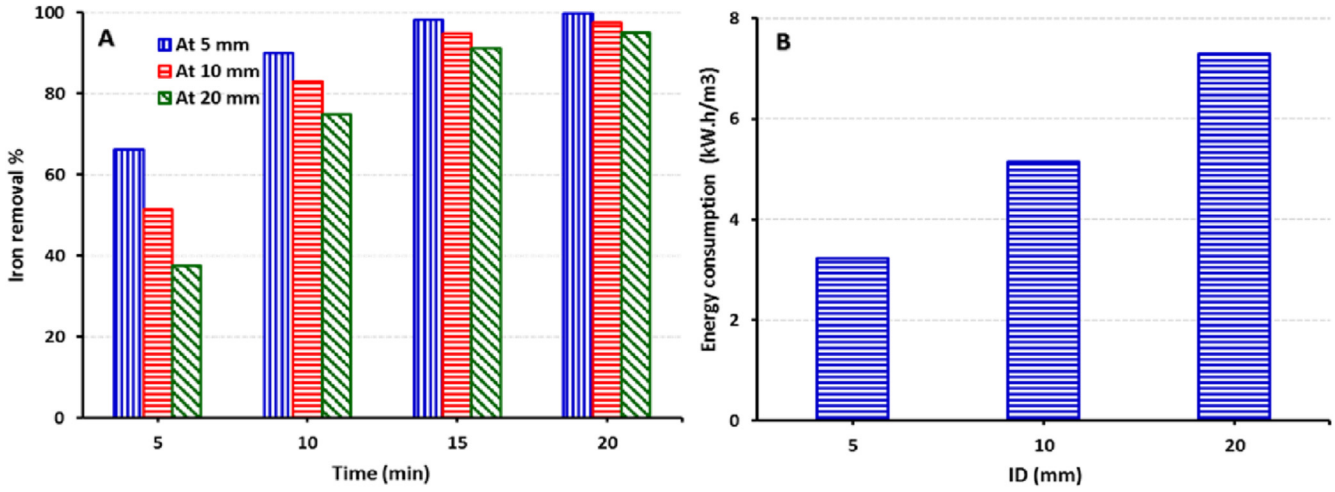


Fig. 4. Effects of ID on: A) iron removal, B) energy consumption.

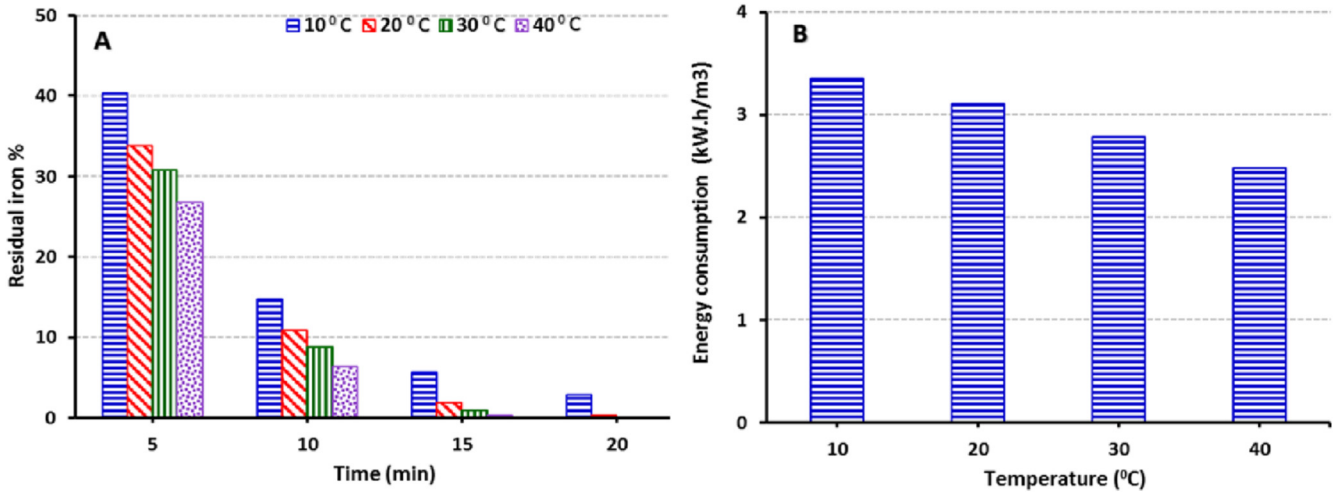


Fig. 5. Effects of water temperature on: (A) iron removal, (B) energy consumption.

energy consumption could be explained by the fact that water viscosity decrease with the increase of temperature, which increases both the number and speed of ions. Therefore the conductivity will likewise increase, hence the energy consumption will change (Barron and Ashton, 2005; Fouad et al., 2009; Gao et al., 2010; Zhao, 2012).

However, it can be concluded from the results obtained that increasing water temperature greater than 20 ^{0}C did not noticeably enhances iron removal and energy consumption. Thus, it is reasonable, in the current study, to adopt the room temperature (20 ^{0}C) to carry out the rest of experiments.

5.1.5. *Influence of initial iron concentration*

The influence of the initial iron concentration on the removal efficiency was explored by electrolysis synthetic water samples with iron concentrations of 20, 40, and 60 mg/L for 45 min at CD of 1.5 mA/cm^2, initial pH of 6, and ID of 5 mm. The variation of the iron removal for the studied initial concentrations is shown in Fig. 6. It can be seen that iron removal noticeably decreased when the initial concentration of iron increased from 20 to 60 mg/L. For instance, it has been found that the residual iron concentration, after 15 min of electrolysis, increased from 16% to about 33% as the initial iron concentration increased from 40 to 60 mg/L, respectively. This could be explained by the availability of the adsorption sites. Where, according to Faraday's law (Equation (24)), a constant quantity of aluminium ions (coagulants) is liberated from the anode for the same CD and electrolysis time, which means, the same quantity of coagulants was produced in the FCER during the removal of the different iron concentrations. Therefore, the formed flocs, at high iron concentrations, were not sufficient to absorb all iron ions, i.e., FCER needs longer time to remove high iron concentrations (>20 mg/L).

It is noteworthy to highlight that although the external mixers and aerators were not used in this new reactor, its ability to remove iron from water was very comparable with those in literature. For instance, Ghosh et al. (2008a) needed about 35 min to remove 99.2% of 25 mg/L of iron from water using an EC cell supplied with magnetic stirrer.

5.2. *Modelling of iron removal*

The variation of iron removal (DV) with the change in the operating parameters (IVs) has been modelled using the multiple regression technique. In this study, SSPS-23 was used to analyse the

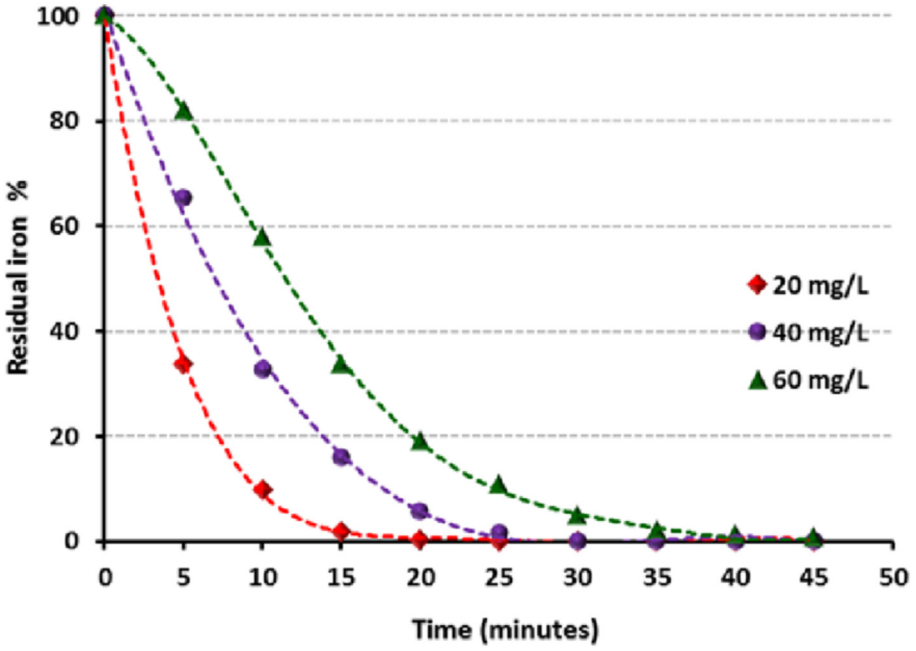


Fig. 6. Effects of initial iron concentration on removal efficiency.

Table 2
Summary of statistical analysis results.

Pollutant	IVs	Tolerance	VIF	Max. detected Mahalanobis distance	Std. residual exceeds the acceptable range (3.0 to −3.0)	
					No. of cases	Value
Iron	*t*	0.998	1.002	17.1	Non	Non
	CD	1.000	1.000			
	C_o	0.988	1.012			
	ID	0.988	1.012			
	pH	0.998	1.002			
	T.	0.998	1.002			

relationship among 107 experimental observations collected from the current study.

Step 1: Check the assumptions of the multiple regression.

In the present investigation, according to Equation 17, the minimum required number of experimental observations to build a generalizable model is 98 observations as six operating parameters (IVs) – duration time, initial pH, CD, ID, T, and C_0 of iron – were experimentally investigated in the current study. The actual measured data points were 107, thus the first assumption has been met. Then, SPSS-23 software was used to perform the required statistical analysis to assess the other main assumptions.

Then, this sample were statistically analysed to check the rest of key assumptions.

The second assumption, which is the multicollinearity among the IVs, has been investigated by calculating the tolerance values for the studied parameters. The results obtained from the collinearity statistics (Table 2) indicate the absence of the multicollinearity phenomenon within the studied observations as calculated tolerance values were greater than 0.1.

Though an initial screening of both the DV and IVs, indicated the absence of the outliers within the experimental observations, the Mahalanobis distances were calculated to detect the existence of outliers. The maximum allowable Mahalanobis distance, according to the critical values listed in Table 1, for six IVs is 22.47. While the maximum calculated Mahalanobis distance, for the experimental observations, was 17.1, which indicates the absence of the outliers.

Finally, the occurrence of normality, linearity, and homoscedasticity of residuals within the studied sample was investigated by calculating the standardised residual values. Where in a normal distribution it is expected that not more than 1% of the standardised residual values of the sample outside the range 3.0 to −3.0. Results of Table 2 confirm that the standardised residual values of the experimental observations were within the permissible range.

Step 2: Evaluating the contribution of each independent variable.

As it has been mentioned before, the statistical significance of each operating parameter determines whether this parameter exerts an important or negligible influence on the outcomes of the suggested model. Where, any parameter with a statistical significance >0.05 could be omitted from the suggested model due its negligible influence.

According to the results obtained from the statistical analysis, the statistical significance of both ID and T were greater than 0.05. Therefore, these two parameters have been omitted from the suggested model.

$$Iron\ Re.\% = \left[1 + \frac{2.35 - 10.89\,CD + 0.024\,t\,C_0 + 2.33\,CD\,pH - 0.14\;C_0\,pH}{C_0}\right] * 100 \tag{25}$$

Beta values for the studied parameters have been calculated in order to measure how strongly each IV influences the outcomes of the built model. Results of Table 3 shows that the influence of the studied operating parameters followed the order: $C_0 > t > CD > pH$.

Step 3: Evaluating the model

After checking the main assumptions of the multiple regression model, the ability of the suggested model to explain the variation in the DV must be assessed by calculating the R^2 value. Here R^2 represents a measure of concordance between the results and estimates generated by the suggested model. The results obtained showed that the R^2, for the suggested model, is 0.86, which is a very acceptable value. Indeed, this R^2 value is comparable with those values calculated by other researchers for different pollutants. For instance, R^2 values for the models of Arulmurugan et al. (2007) and Adebayo et al. (2015) were 0.85 and 0.893, respectively. Another important factor that must be checked in this step is the statistical significance of the suggested model (*Sig.*), which must be less than 0.05 to accept the suggested model (Pallant, 2005).

The *Sig.* of the suggested model was 0.000, which indicates the applicability of the suggested model to reproduce the performance of the FCER in terms of iron removal from water within the studied values of the operating parameters.

To investigate the agreement between the predicted and measured removal efficiencies, the suggested model has been applied to a randomly selected set of experimental data consisting of 50 observations obtained under different operating conditions. This tests the ability of the suggested model to reproduce the iron removal performance of the FCER within the studied values of the operating parameters.

The results obtained, Fig. 7, indicated a good agreement between the predicted and experimental iron removal, where the R^2 value, for this randomly selected observations, was 0.837.

Basing on the results obtained from this validation, it could be said that the suggested empirical model is applicable to predict the performance of FCER in terms of iron removal from drinking water within the studied values of the operating parameters.

5.3. Operating cost (OC)

Operating cost, as mentioned before, is a fundamental consideration in any treatment method as it determines the real-world applicability of that method. In this economic investigation, the operating cost for iron removal from drinking water was calculated according to the unit prices of the Iraqi market in August 2015 (2.5 pence/kWh of electricity, and 1.53$/kg of aluminium).

The magnitude of the consumed energy, according to Equation (12), was 3.2 kWh/m^3. While, the consumed amount of material of electrodes was calculated using Equation (24). Then, the minimum cost for iron removal in this project is:

$$OC = 3.2 * 2.5/100 + 1.53 * 0.091 = 0.22 \text{ US \$/m}^3$$

This cost is very comparable with that obtained, for EC method, by other researchers. For instance (Kobya et al., 2010), found that the required cost to treat cadmium-cyanide and nickel-cyanide containing effluents, using EC cell, at a current density of 5 A/m^2 was about 0.186 €/m^3 (0.2 $/m^3).

It noteworthy that although the operating cost of FCER was comparable those in literature, FCER has reduced the need for external mixing and aeration devices which required extra power to work; these devices until now have been widely used in the EC reactors (especially laboratory scale ones). Therefore, FCER could be a cost-effective alternative to the traditional lab-scale EC reactors.

In fact, additional costs such as labour, consumed chemicals, maintenance, and sludge-handling must be taken into consideration for the commercial use of the EC method.

Table 3
Beta values for the studied parameters.

IVs	Beta
t	0.519
CD	0.076
C_o	0.700
pH	0.075
ID	Omitted
T	Omitted

5.4. Estimating the produced hydrogen gas and the yieldable energy from this gas

The quantification of H_2 gas emission from the FCER, during the electrolysis of iron containing water, was carried out using Equation (21). According to the results obtained from experimental work, the required electrolysis time to remove 60 mg/L of iron from water, at CD of 1.5 mA/cm^2, is about 45 min. Therefore, the produced amount of H_2 gas is:

$$Q_{H_2} = \frac{15 * 0.0284 * 2700 * 0.5}{96500} = 0.006 \text{ mole} = 0.144 \text{ L}$$

Then the yieldable energy from this amount of H_2 gas, according to Equation (22), is 1.46 *10^{-3} MJ, which equivalent to 10.14 kW/m^3. In fact, according to these results, the harvested amount of H_2 gas from filed-scale EC plants could be used to generate a considerable amount of energy.

5.5. Scanning electron microscopy characterisation of electrodes

In order to investigate the influence of the EC process on the morphology of anode surface, SEM images of aluminium anode, before and after EC process, were obtained. The generated images, indicated that the virgin anode surface was uniform and homogenous except small scratches (Fig. 8-(A)), which could have happened due to mechanical handling of metal during electrode shaping process. Fig. 8-(B) shows the same anode after a series of EC experiments. The anode surface became inhomogeneous, with several dents. This could be attributed to the consumption of anode material at the active sites where the anode dissolution results in the generation of aluminium hydroxides (coagulation ions) (Ahlawat et al., 2008; Vasudevan et al., 2012a).

6. Conclusion

The current project was curried out to show that non-traditional EC reactors could be used for economic and efficient removal of water pollutants. In this study, a new EC reactor, FCER, has been applied to remove iron from drinking water taking into consideration the influence of key operating parameters. The obtained results showed that iron removal is more efficient in the neutral pH levels, and the coagulants produced from the sacrificial anode is proportional to combination of both CD and electrolysis duration, which in turn influences iron removal. Contrarily, iron removal is reversely proportional to the C_0 and ID. In addition, it was found that the EC process generates a considerable amount of H_2 gas that could be used as an eco-friendly fuel in different applications.

Statistically, it has been found that the influence of the studied operating parameters on iron removal could be modelled with R^2 of 0.86.

In conclusion, basing on the obtained results, FCER could be an

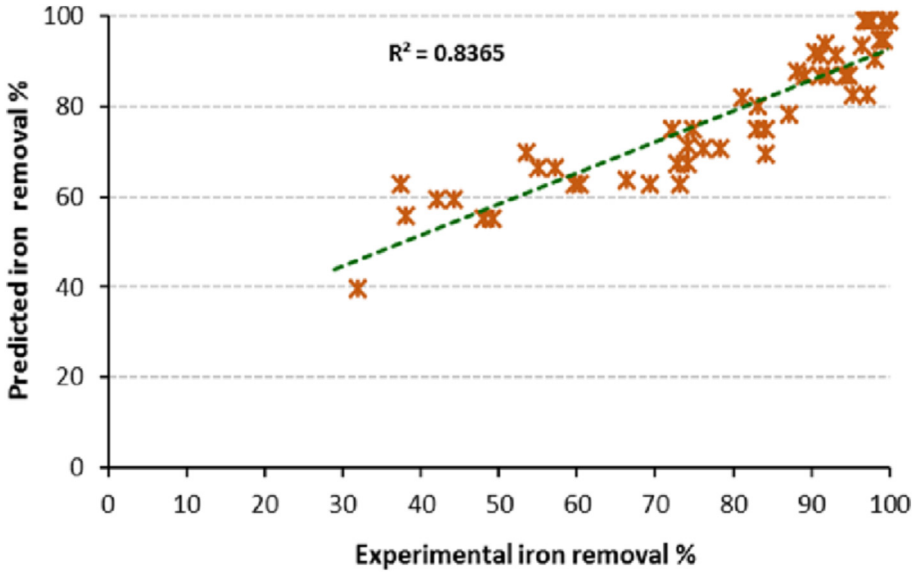


Fig. 7. Experimental vs predicted iron removal for randomly selected data points.

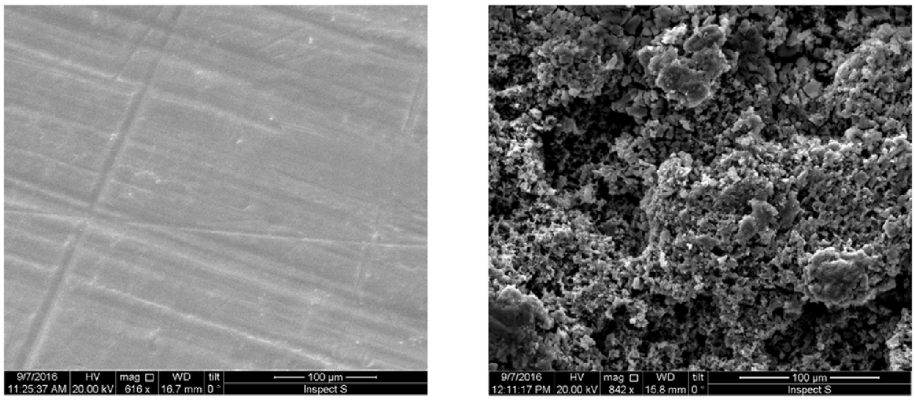


Fig. 8. SEM images of aluminium anode, (A) before EC process, and (B) After EC process.

efficient and cost-effective alternative to the traditional lab-scale EC cells as it reduced the need for external stirring and aerating devices that required extra power to work.

For future work, the new EC reactor should be used to remove other pollutants, such as arsenic and nitrate, from water and wastewater. Additionally, an SEM investigation should be carried out to characterise the produced sludge from this new reactor, which will further enlighten on the reactions taken place.

Acknowledgement

This project was supported by the Iraqi Ministry of Higher Education and Scientific Research, Babylon University. I thank my colleagues and the technician team from Liverpool John Moores University, United Kingdom, who provided insight and expertise that greatly assisted the project as and when required.

References

Adebayo, S.B., Tawabini, B.S., Atieh, M.A., Abuilaiwi, F.A., Alfadul, S., 2015. Investigating the removal of methyl tertiary butyl ether (MTBE) from water using raw and modified fly ash waste materials. In: The 14th International Conference on Environmental Science and Technology. Rhodes, Greece.

Adhoum, N., Monser, L., Bellakhal, N., Belgaied, J.E., 2004. Treatment of electroplating wastewater containing Cu2+, Zn2+ and Cr(VI) by electrocoagulation. J. Hazard Mater. 112, 207–213.

Aghdam, M.A., Kariminia, H.-R., Safari, S., 2015. Removal of lignin, COD, and color from pulp and paper wastewater using electrocoagulation. Desalination Water Treat. 57, 9698–9704.

Ahlawat, R., Srivastava, V.C., Mall, I.D., Sinha, S., 2008. Investigation of the electrocoagulation treatment of cotton blue dye solution using aluminium electrodes. Clean. - Soil, Air, Water 36, 863–869.

Arulmurugan, A., Chithra, K., Thilakavathi, R., Balasubramanian, N., 2007. Degradation of textile effluent by electro coagulation technique. Bull. Electrochem. 23, 247–252.

Attour, A., Touati, M., Tlili, M., Ben Amor, M., Lapicque, F., Leclerc, J.P., 2014. Influence of operating parameters on phosphate removal from water by electrocoagulation using aluminum electrodes. Sep. Purif. Technol. 123, 124–129.

Barron, J.J., Ashton, C., 2005. The effect of temperature on conductivity measurement. TSP 7. http://www.camlabworld.com/originalimages/sitefiles/Tech_papers/TempCondMeas.pdf.

Chaturvedi, S., Dave, P.N., 2012. Removal of iron for safe drinking water. Desalination 303, 1–11.

Chaturvedi, S.I., 2013. Electrocoagulation: a novel waste water treatment method. Int. J. Mod. Eng. Res. 3, 93–100.

Daneshvar, N., Sorkhabi, H.A., Kasiri, M.B., 2004. Decolorization of dye solution containing Acid Red 14 by electrocoagulation with a comparative investigation of different electrode connections. J. Hazard Mater. 112, 55–62.

Deokate, A., 2015. Development of textile waste water treatment reactor to obtain drinking water by solar powered electro-coagulation technique. Int. J. Res.

Environ. Sci. Technol. 5, 29–34.
Eker, S., Kargi, F., 2010. Hydrogen gas production from electrohydrolysis of industrial wastewater organics by using photovoltaic cells (PVC). Int. J. Hydrogen Energy 35, 12761–12766.
El-Naas, M.H., Al-Zuhair, S., Al-Lobaney, A., Makhlouf, S., 2009. Assessment of electrocoagulation for the treatment of petroleum refinery wastewater. J. Environ. Manag. 91, 180–185.
Emamjomeh, M.M., Sivakumar, M., 2005. Electrocoagulation (EC) technology for nitrate removal. In: The 9th Annual Environmental Research Event (ERE) Conference. Tasmania, Australia.
Emamjomeh, M.M., Sivakumar, M., 2009. Fluoride removal by a continuous flow electrocoagulation reactor. J. Environ. Manag. 90, 1204–1212.
Essadki, A.H., Gourich, B., Vial, C., Delmas, H., Bennajah, M., 2009. Defluoridation of drinking water by electrocoagulation/electroflotation in a stirred tank reactor with a comparative performance to an external-loop airlift reactor. J. Hazard Mater. 168, 1325–1333.
Fouad, Y.O.A., Konsowa, A.H., Farag, H.A., Sedahmed, G.H., 2009. Performance of an electrocoagulation cell with horizontally oriented electrodes in oil separation compared to a cell with vertical electrodes. Chem. Eng. J. 145, 436–440.
Gao, S., Yang, J., Tian, J., Ma, F., Tu, G., Du, M., 2010. Electro-coagulation-flotation process for algae removal. J. Hazard Mater. 177, 336–343.
Gao, Y., Zhou, Y., Wang, H., Lin, W., Wang, Y., Sun, D., Hong, J., Li, Q., 2013. Simultaneous silver recovery and cyanide removal from electroplating wastewater by pulse current electrolysis using static cylinder electrodes. Ind. Eng. Chem. Res. 52, 5871–5879.
García-García, A., Martínez-Miranda, V., Martínez-Cienfuegos, I.G., Almazán-Sánchez, P.T., Castañeda-Juárez, M., Linares-Hernández, I., 2015. Industrial wastewater treatment by electrocoagulation–electrooxidation processes powered by solar cells. Fuel 149, 46–54.
Genc, A., Bakirci, B., 2015. Treatment of emulsified oils by electrocoagulation: pulsed voltage applications. Water Sci. Technol. 71, 1196–1202.
Ghosh, D., Solankiand, H., Purkait, M.K., 2008a. Removal of Fe(II) from tap water by electrocoagulation technique. J. Hazard Mater. 155, 135–143.
Ghosh, D., Medhi, C.R., Purkait, M.K., 2008b. Treatment of fluoride containing drinking water by electrocoagulation using monopolar and bipolar electrode connections. Chemosphere 73, 1393–1400.
Ghosh, D., Medhi, C.R., Purkait, M.K., 2011. Techno-economic analysis for the electrocoagulation of fluoride-contaminated drinking water. Toxicol. Environ. Chem. 93, 424–437.
Ghosh, D., Sinha, M.K., Purkait, M.K., 2013. A comparative analysis of low-cost ceramic membrane preparation for effective fluoride removal using hybrid technique. Desalination 327, 2–13.
Ityel, D., 2011. Ground water: dealing with iron contamination. Filtr. Sep. 48, 26–28.
Kamaraj, R., Vasudevan, S., 2015. Evaluation of electrocoagulation process for the removal of strontium and cesium from aqueous solution. Chem. Eng. Res. Des. 93, 522–530.
Khandegar, V., Saroha, A.K., 2013. Electrocoagulation for the treatment of textile industry effluent–a review. J. Environ. Manag. 128, 949–963.
Kobya, M., Demirbas, E., Akyol, A., 2009. Electrochemical treatment and operating cost analysis of textile wastewater using sacrificial iron electrodes. Water Sci. Technol. 60, 2261–2270.
Kobya, M., Demirbas, E., Parlak, N.U., Yigit, S., 2010. Treatment of cadmium and nickel electroplating rinse water by electrocoagulation. Environ. Technol. 31, 1471–1481.
Kuokkanen, V., 2016. Utilization of Electrocoagulation for Water and Wastewater Treatment and Nutrient Recovery. Techno-economic studies. (Ph.D. thesis). University of Oulu Graduate School; University of Oulu.
Lakshmi, J., Sozhan, G., Vasudevan, S., 2013. Recovery of hydrogen and removal of nitrate from water by electrocoagulation process. Environ. Sci. Pollut. Res. 20, 2184–2192.
Lim, K.F., 2006. Negative pH does exist. J. Chem. Educ. 83, 1465.
Mameri, N., Yeddou, A.R., Lounici, H., Belhocine, D., Grib, H., Bariou, B., 1998. Defluoridation of septentrional sahara water of north africa by electrocoagulation process using bipolar aluminium electrodes. Wat. Res. 32, 1604–1612.
Maximova, N., Dahl, O., 2006. Environmental implications of aggregation phenomena: current understanding. Curr. Opin. Colloid & Interface Sci. 11, 246–266.
Mohora, E., Roncevic, S., Dalmacija, B., Agbaba, J., Watson, M., Karlovic, E., Dalmacija, M., 2012. Removal of natural organic matter and arsenic from water by electrocoagulation/flotation continuous flow reactor. J. Hazard Mater. 235-236, 257–264.
Mustapha, A., Abdu, A., 2012. Application of principal component analysis & multiple regression models in surface water quality assessment. J. Environ. Earth Sci. 2, 16–23.
Nasution, M.A., Yaakob, Z., Ali, E., Tasirin, S.M., Abdullah, S.R., 2011. Electrocoagulation of palm oil mill effluent as wastewater treatment and hydrogen production using electrode aluminum. J. Environ. Qual. 40, 1332–1339.
O'brien, R.M., 2007. A caution regarding rules of thumb for variance inflation factors. Qual. Quantity 41, 673–690.
Ozyonar, F., Karagozoglu, B., 2011. Operating cost analysis and treatment of domestic wastewater by electrocoagulation using aluminum electrodes. Pol. J. Environ. Stud 20, 173–179.
Pallant, J., 2005. SPSS Survival Manual. Allen & Unwin, Australia.
Phadke, A., 2014. Iron Removal Using Electro- Coagulation Followed by Floating Bead Bed Filtration (MSc thesis). Louisiana State University and Agricultural and Mechanical College.
Phalakornkule, C., Sukkasem, P., Mutchimsattha, C., 2010. Hydrogen recovery from the electrocoagulation treatment of dye-containing wastewater. Int. J. Hydrogen Energy 35, 10934–10943.
Song, S., He, Z., Qiu, J., Xu, L., Chen, J., 2007. Ozone assisted electrocoagulation for decolorization of C.I. Reactive Black 5 in aqueous solution: an investigation of the effect of operational parameters. Sep. Purif. Technol. 55, 238–245.
Tabachnick, B.G., Fidell, L.S., 2001. Using Multivariate Statistics. Allyn and Bacon, Boston.
Un, U.T., Koparal, A.S., Bakir Ogutveren, U., 2009. Electrocoagulation of vegetable oil refinery wastewater using aluminum electrodes. J. Environ. Manag. 90, 428–433.
Un, U.T., Koparal, A.S., Bakir Ogutveren, U., 2013. Fluoride removal from water and wastewater with a bach cylindrical electrode using electrocoagulation. Chem. Eng. J. 223, 110–115.
Vasudevan, S., Lakshmi, J., Sozhan, G., 2012a. Optimization of electrocoagulation process for the simultaneous removal of mercury, lead, and nickel from contaminated water. Environ. Sci. Pollut. Res. 19, 2734–2744.
Vasudevan, S., Lakshmi, J., Sozhan, G., 2012b. Optimization of the process parameters for the removal of phosphate from drinking water by electrocoagulation. Desalination Water Treat. 12, 407–414.
Vasudevan, S., Lakshmi, J., Sozhan, G., 2012c. Simultaneous removal of Co, Cu, and Cr from water by electrocoagulation. Toxicol. Environ. Chem. 94, 1930–1940.
Vepsäläinen, M., Ghiasvand, M., Selin, J., Pienimaa, J., Repo, E., Pulliainen, M., Sillanpää, M., 2009. Investigations of the effects of temperature and initial sample pH on natural organic matter (NOM) removal with electrocoagulation using response surface method (RSM). Sep. Purif. Technol. 69, 255–261.
World Health Organization, 2004. Guidelines for Drinking Water Quality, Recommendations, 3rd ed. World Health Organization, Geneva.
Woody, A.I., 2011. How is the ideal gas law explanatory? Sci. Educ. 22, 1563–1580.
Ye, S., 2016. Comparison of electrochemical treatment of petroleum refinery effluents using electrooxidation, electrocoagulation and electrophenton process. Int. J. Electrochem. Sci. 6173–6182.
Yilmaz, A.E., Boncukcuoglu, R., Kocakerim, M.M., Yilmaz, M.T., Paluluoglu, C., 2008. Boron removal from geothermal waters by electrocoagulation. J. Hazard Mater 153, 146–151.
Zaroual, Z., Chaair, H., Essadki, A.H., El Ass, K., Azzi, M., 2009. Optimizing the removal of trivalent chromium by electrocoagulation using experimental design. Chem. Eng. J. 148, 488–495.
Zhao, S., 2012. Forward Osmosis for Desalination and Water Treatment: a Study of the Factors Influencing Process Performance. PhD thesis University of South Australia.
Zhu, J., Zhao, H., Ni, J., 2007. Fluoride distribution in electrocoagulation defluoridation process. Sep. Purif. Technol. 56, 184–191.